



Heat transfer and pressure drop performance evaluation of twisted and bent fins when steam flows through the tubes[☆]

Hao Zhou^{*}, Tianxiao Liu, Fangzheng Cheng, Dan Liu, Yifan Zhu, Weiwei Ma

State Key Laboratory of Clean Energy Utilization, Institute for Thermal Power Engineering, Zhejiang University, Hangzhou 310027, China

ARTICLE INFO

Article history:

Received 15 October 2021

Revised 16 November 2021

Accepted 27 November 2021

Available online 9 December 2021

Keywords:

Bent serrated fin

Heat transfer enhancement

Pressure drop

Superheated steam

ABSTRACT

In this investigation, the heat transfer and resistance characteristics of the serrated helical finned tube under steam in tube condition were studied. Based on the traditional serrated spiral finned tube, a bent serrated spiral finned tube was proposed. The performances of bent and non-bent finned tubes were compared under two different pitches (4.23 and 6.35 mm). At the same time, the effects of steam flow rate on heat transfer and resistance characteristics of heat exchangers were tested. The results showed that the bent fins could increase the heat transfer rate and pressure drop by improving the turbulence intensity on the flue gas side compared with the ordinary fins with the same area. Under the same Re , the increase of steam flow could enhance the heat transfer performance, but the flue gas side pressure drop was basically unchanged. Through the overall performance evaluation, it was concluded that the bent fin with a small fin pitch had better performance, 15.18–17.05% higher than that of traditional serrated spiral finned tube. Finally, the correlation for Colburn factor (j) and friction factor (f) was fitted to provide suggestions for engineering practice.

© 2021 Elsevier Ltd. All rights reserved.

1. Introduction

As we all know, the finned tube heat exchanger is widely used in the chemical industry, air conditioning, electric power and other industries because of its compact structure and high heat exchange efficiency. As one of the key units of the heat exchanger, the improvement of finned tube performance is significant to heat exchange. Due to the high thermal resistance of the air-side, the transformation of the air-side fin is one of the leading research directions at present. Many researchers have investigated the improvement of the fin, including tube layout and fin geometry [1–3]. At present, there have been many studies on fin shape, such as three-dimensional fin [4, 5], H-shaped fin [6, 7], louver fin [8], spiral fin [9], etc. Among them, the spiral fin is the most widely used in engineering due to its excellent performance. Researchers have conducted extensive research on spiral finned tubes.

He et al. [10] carried out experimental research on 13 kinds of spiral finned tube bundle heat exchangers with fixed outer diameter of the tube, different fin pitches and fin heights and obtained the Nu correlation and Eu correlation with Re , fin pitch, fin height, transverse and longitudinal tube pitch. They concluded that the

Nu increased with the increase of Re and transverse tube pitch; decreased with the increase of longitudinal tube pitch. Lee et al. [11] gained the empirical correlation of the j factor related to Re and the tube row number by changing the fin spacing, the tube row amount and the fin arrangement. Due to higher flow mixing activated by the horseshoe vortex around the fins and tubes, the heat transfer performance heat exchangers with the staggered fin alignment were higher than those with the inline fin alignment.

Based on the spiral finned tube, a serrated finned tube with better heat transfer efficiency is developed. The serrated spiral finned tube has high turbulence intensity, so it has better heat transfer and greater resistance. Næss [12] studied the influence of tube bundle layouts, tube and fin parameters on heat transfer and resistance of serrated spiral finned tubes. When the flow areas of the cross and oblique section were the same, the heat transfer coefficient reached the maximum. Weierman [13], Chen [14], Zhou et al. [15] and Ma et al. [16] all explored the influence of spiral fin spacing on heat transfer and resistance performance of heat exchangers and gave relevant performance correlations.

In addition to serrated finned tubes, bending spiral finned tubes based on spiral finned tubes has also been widely studied. The curved finned tube can also increase the heat transfer efficiency on the flue gas side. Pongsoi et al. [17] investigated the air-side properties of curved helical fins and tubular heat exchangers made of copper and aluminum with various rows of tubes ($N_{row} = 2, 3, 4$ and 5), and tested the influence of tube rows and fin mate-

[☆] Permanent Postal Address: State Key Laboratory of Clean Energy Utilization, Zhejiang University, Zheda Road 38, Hangzhou 310,027, China

^{*} Corresponding author.

E-mail address: zhouhao@zju.edu.cn (H. Zhou).

Nomenclature

A_i	tube inside surface area, m^2
A_f	fin surface area of the finned tube bundle, m^2
A_{min}	minimum free flow area, m^2
A_o	frontal area, m^2
A_t	bare tube surface area, m^2
A_{tot}	total outside surface area part of the finned tube bundle, m^2
C_p	specific heat at constant pressure, $J/(kg \cdot K)$
d_i	inner diameter of the tube, mm
d_o	outer diameter of the tube, mm
d_f	outer diameter of fin, mm
Eu	Euler number, dimensionless $Eu = \Delta P / \rho v^2$
f	Fanning friction factor, dimensionless
G_C	gas mass flux in the minimum free flow area, $kg/(m^2 \cdot s)$
h	Fin height, mm
j	Colburn heat transfer factor
K	overall heat transfer coefficient, $W/(m^2 \cdot K)$
N_{row}	tube numbers in gas flow direction
Nu	Nusselt number, dimensionless $Nu = \alpha \cdot d / \lambda$
Pr	Prandtl number, dimensionless
p_f	fin pitch, mm
Q_{ave}	average heat transfer rate, kW
Re	Reynolds number based on tube outside diameter, dimensionless
S_D	diagonal tube pitch, mm
S_L	longitudinal tube pitch, mm
S_T	transverse tube pitch, mm
V_{max}	maximum velocity across heat exchanger, m/s
<i>Greek symbols</i>	
α_i	tube side heat transfer coefficient, $W/(m^2 \cdot K)$
α_o	fin side (external side) heat transfer coefficient, $W/(m^2 \cdot K)$
β	deflection angle, $^\circ$
η_f	actual fin efficiency
δ	fin thickness, mm
δ_t	tube wall thickness, mm
λ_s	thermal conductivity of superheated steam, $W/(m \cdot K)$
λ_t	thermal conductivity of tube, $W/(m \cdot K)$
ρ	density, kg/m^3
ΔP	pressure drop, Pa
Δt_m	logarithmic mean temperature difference for counter-current flow, $^\circ C$
σ	ratio of minimum free flow area to frontal area
<i>Subscripts</i>	
1, 2	flue gas inlet, flue gas outlet
g, s	flue gas, steam
i, o	tube inside, tube outside
f	fin
t	tube
w	wall
0	constant property case
b	evaluated at local bulk temperature;
<i>Abbreviations</i>	
BSSF	bent serrated spiral fin
SSF	serrated spiral fin

rials on heat transfer and friction properties. They found the air-side performance was independent of fin material, and the aver-

age heat transfer rate and pressure drop increased with increasing the number of tube rows. Nuntaphan et al. [18, 19] studied the heat transfer performance of curved finned tubes under dehumidification and without dehumidification, respectively, and found that the heat transfer properties of the dry surface were stronger. They also found the effect of the fin pitch on the airside performance is strongly related to the transverse tube pitch and gave the performance correlation of crimped spiral fins in both staggered and inline arrangements.

Although many researchers have studied serrated finned and curved finned tubes, respectively, there is no research combining the two kinds of fins. Therefore, this paper combines the serrated finned and the curved finned tube, and puts forward the serrated twisted and bent finned tube. In practical engineering applications, it is necessary to use steam as the medium in the tube to exchange heat with high-temperature flue gas to improve the steam enthalpy, but the research on that is relatively lacking. Therefore, the heat transfer and pressure drop performance of the heat exchanger with the bent serrated spiral finned tube under steam in the tube were studied in this paper. According to the experimental results, the correlation between heat transfer and resistance characteristics was proposed.

2. Experimental system and procedure

The diagrammatic drawing of the experimental setting is displayed in Fig. 1. The working fluids were flue gas and superheated steam. The principal parts of the system included the flue gas feed system, steam generation system, heat exchanger, test instrumentation and data collection system.

The flue gas feed system consisted of the induced draft fan of the centrifugal and oil-fired boiler. The hot flue gas was passed through the heat exchanger by an open wind tunnel. Both the tunnel and heat exchanger were covered by thermal insulation material to decrease the heat loss. The high-temperature smoke produced by the oil combustion was led by an induced draft fan with a main blade speed of 1450 r/min and a rated power of 45 kW. A guide plate was placed in the flue behind the hot blast stove to make the flue gas flow at the inlet of the heat exchanger stable and the velocity distribution uniform. The flue gas entered the finned tube group in the test section through the inlet channel, and transferred heat with superheated steam in the tube. The flue gas temperature and flow rate were adjusted by changing the load of the oil-burning boiler and the opening of the baffle in the air duct, respectively.

The steam generation system consisted of a water softener, steam boiler and steam superheater. The tap water entered the steam boiler water tank after being purified by the water softener. The water was heated into saturated steam by the boiler and then discharged. After being heated again by the steam superheater, it became superheated steam and then entered the heat exchanger. The steam was released to the wastewater tank after heat exchange with hot flue gas.

The present study analyzed heat exchangers with two fin patterns, the serrated spiral fin (SSF) and the bent serrated spiral fin (BSSF), shown in Fig. 2, each of them having two fin pitches: 4.23 and 6.35 mm. BSSF was made by twisting all fins of SSF and bending every other fin at a certain angle. Except that, the two fin structures with the same fin pitch were precisely the same, and the specific parameters were shown in Table 1.

The photos of BSSF and SSF are presented in Fig. 3. The tubes and fin were made from carbon steel. The contact thermal resistance between them can be neglected because the fin foot was welded to the tube by high-frequency resistance welding.

Fig. 4 shows the arrangement of finned tubes. Each heat exchanger had 10 rows of pipelines, with each row of 8 finned tubes.

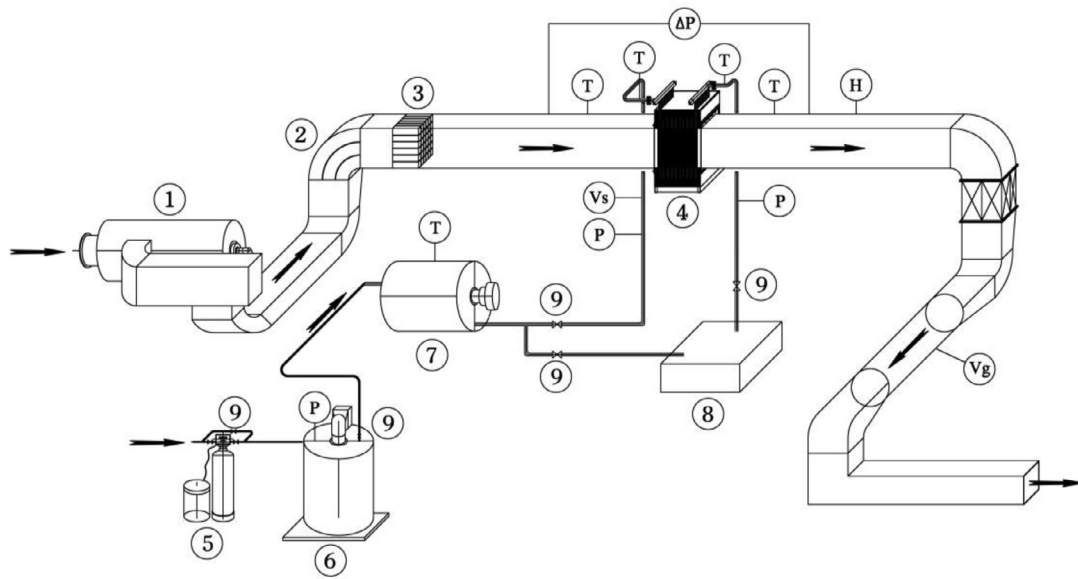


Fig. 1. Schematic diagram of the experimental apparatus. ① diesel boiler ② deflectors ③ straightener ④ heat transfer section ⑤ water softener ⑥ steam boiler ⑦ steam superheater ⑧ waste water pool ⑨ valves.

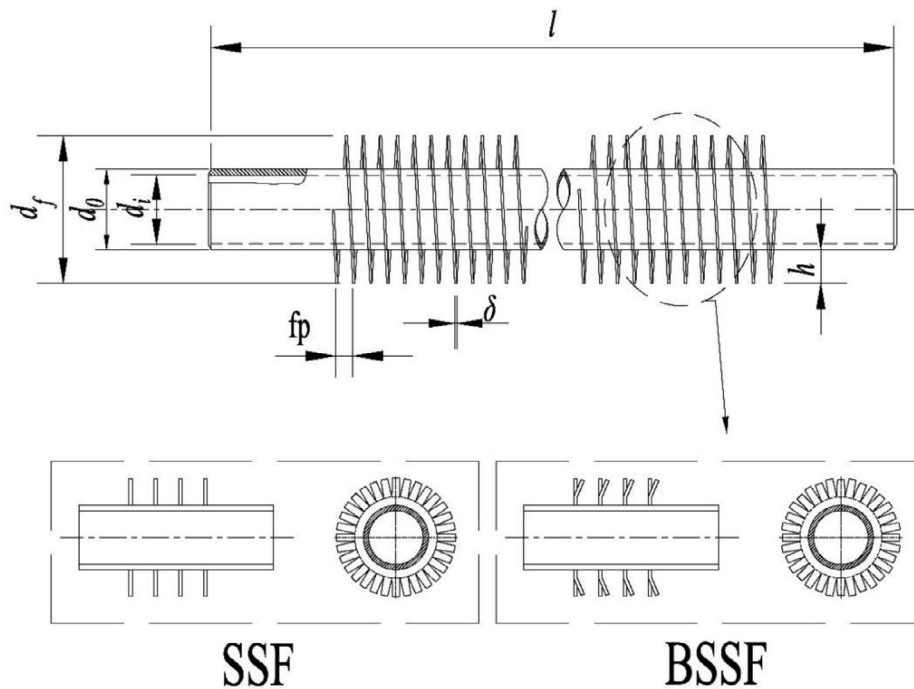


Fig. 2. Schematic diagram of serrated spiral fin and bent serrated spiral fin.

For better heat exchange efficiency, high-temperature flue gas and superheated steam conducted countercurrent heat exchange. The superheated steam was divided in a DN50 pipeline through the diverter before entering the heat exchanger for heat exchange with hot steam.

The measurement system is shown in Fig. 1. The inlet and outlet temperature of flue gas were tested by K-type thermocouples arranging in a 4×3 grid. The flue gas composition was divided into dry flue gas composition and flue gas humidity, which were measured by the testo 350 flue gas analyzer and the Janapo HMS545P portable flue gas moisture meter, respectively. The flue gas flow was detected by the downstream S-type Pitot tube in the experimental section. Four pressure measuring ports connected in

parallel were arranged at the front and rear of the heat exchanger, and the pressure difference of the flue gas between the inlet and outlet of the heat exchange section was obtained by testo 435-4 multi-functional measuring instrument. The inlet and outlet temperature and pressure of superheated steam were measured by K-type thermocouple and pressure gage, respectively. The mass flow of steam was recorded by an orifice flowmeter with an outflow coefficient of 0.61. All of the measuring apparatus was referred to be calibrated.

When the temperature of each thermocouple is stable within ± 0.25 °C and the average pressure per half a minute is stable within ± 0.1 Pa, the system is deemed to be stable. All data was recorded at 5-seconds intervals for about 10 min. In a typical run, the flue

Table 1
Detailed geometric parameters of the test fin tube.

NO.	Fin type	d_i (mm)	d_o (mm)	d_f (mm)	f_p (mm)	S_L (mm)	S_T (mm)	N_{row}	S_f (mm)	Bent and twist
1	BSSF	26.6	32	64	4.23	71	83	10	3.43	yes
2	SSF	26.6	32	64	4.23	71	83	10	2	no
3	BSSF	26.6	32	64	6.35	71	83	10	5.55	yes
4	SSF	26.6	32	64	6.35	71	83	10	3	no

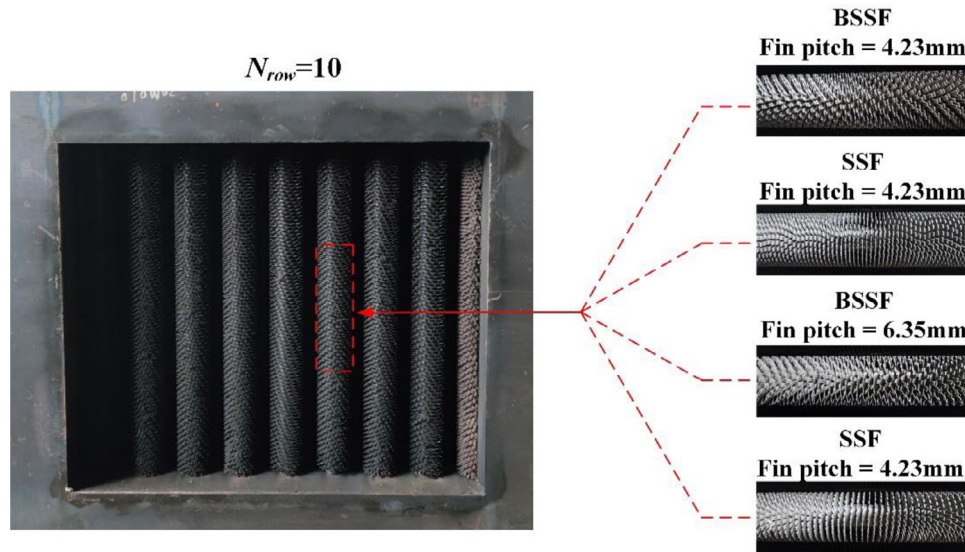


Fig. 3. The photo of serrated spiral fin and bent serrated spiral fin.

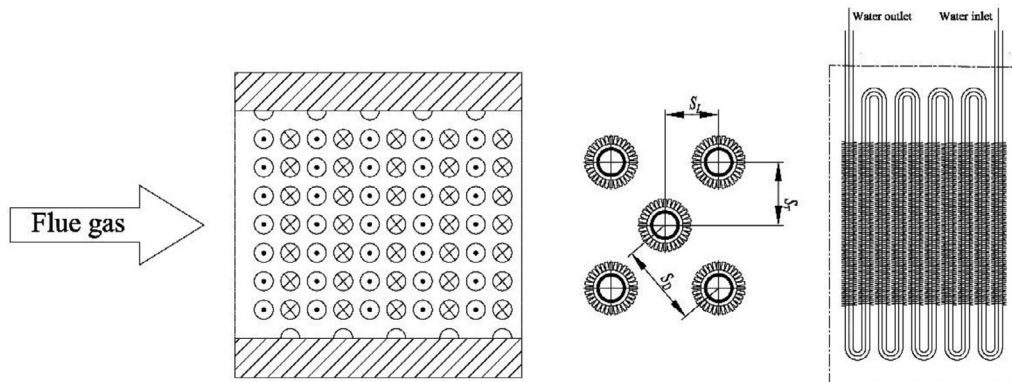


Fig. 4. Arrangement of finned tube bundles.

Table 2
Experimental conditions.

Inlet flue gas temperature, °C	300
flue gas velocity, m/s	7 ~ 15
Inlet steam temperature, °C	165
Inlet steam pressure, MPa	0.4
Inlet steam flow rate, m/s	16 ~ 27

Table 3
The accuracies of the measurements.

Parameters	Accuracy
Inlet flue gas temperature, °C	± 0.5
Pressure drop, Pa	± 1
Inlet steam temperature, °C	± 0.5
Flue gas moisture meter	± 2% of full scale
Inlet steam flow rate	± 1.136% of full scale

gas flow rate increased when the steam was stable, and the flue gas temperature was settled. The working conditions of the experiment, set according to the actual situation of industrial production, are shown in Table 2.

3. Data reduction

For the convenience of calculation, the flue gas in this experiment was viewed as perfect gas of nitrogen, oxygen, carbon diox-

ide and steam. The thermophysical properties of flue gas such as density, specific heat capacity and kinematic viscosity were obtained according to the empirical formula [20]. The thermophysical properties of superheated steam can be obtained from IAPWS-IF97 [21]. According to the thermophysical properties of the two, the flow gas side heat transfer (Q_g) and steam side heat transfer (Q_s) can be obtained. The average heat transfer Q_{ave} is averaged from

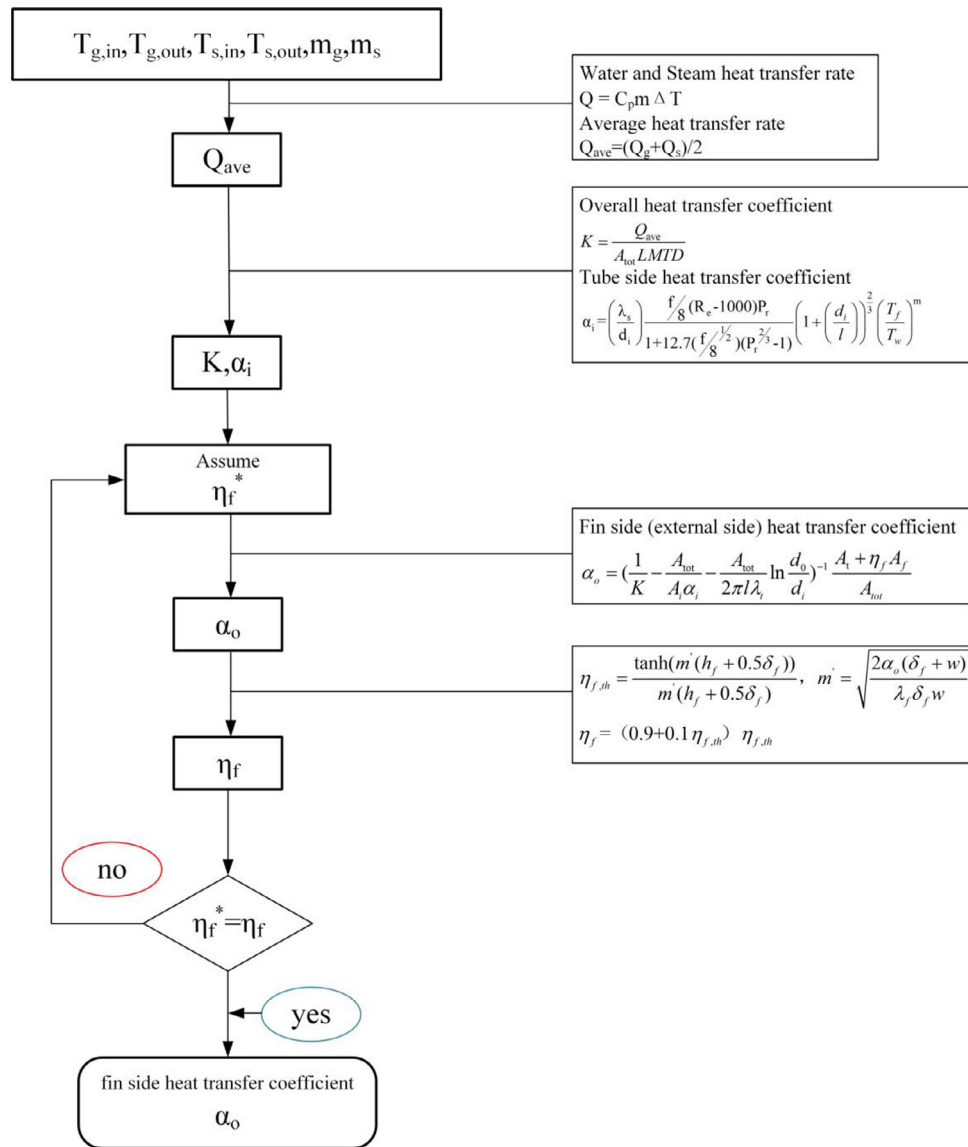


Fig. 5. Flowchart of the data reduction for air-side heat transfer coefficient.

Q_g and Q_s as follows:

$$Q_{ave} = \frac{|Q_g| + |Q_s|}{2} \quad (1)$$

The overall heat transfer coefficient K is given as:

$$K = \frac{Q_{ave}}{A_{tot} \Delta t_m} \quad (2)$$

in which A_{tot} represents the total heat exchange area of the flue gas side. Δt_m is the log mean temperature difference (LMTD).

$$LMTD = \frac{\Delta T_{max} - \Delta T_{min}}{\ln(\Delta T_{max} / \Delta T_{min})} \quad (3)$$

The flue gas side heat transfer coefficient α_o can be calculated as

$$\alpha_o = \left[\left(\frac{1}{K} - \frac{\delta_t A_{tot}}{\lambda_t A_m} - (\alpha_i + R_{fi}) \frac{A_{tot}}{A_i} \right) \frac{(A_t + \eta_f A_f)}{A_{tot}} - R_{fo} \right]^{-1} \quad (4)$$

where R_{fi} and R_{fo} are the fouling factors of the tube inside and outside, respectively. In this experiment, the flue gas was produced by clean diesel so that it could be ignored. δ_t represents the base tube wall thickness. λ_t represents the thermal conductivity of the base

tube, which is 48 W/(m·K) in this study [22]. A_i, A_t, A_m, A_f are the internal surface area of the tube, the surface area of the bare tube according to the outside diameter of the base tube, bare tube surface area according to the average diameter of the base tube, fin surface area, respectively. η_f represents the fin efficiency corrected by the Weierman method [13]. α_i is the tube side heat transfer coefficient, can be obtained by Gnielinski's correlation [23]. This relation expression has been widely certified [24, 25]. The calculation equation is as follows:

$$Nu_{0,i} = \frac{\alpha_i d_i}{\lambda_s} = \frac{(f_i/8)(Re_i - 1000)Pr_i}{1 + 12.7\sqrt{(f_i/8)}(Pr_i^{2/3} - 1)} \left(1 + \left(\frac{d_i}{l} \right)^{0.4} \right) \quad (5)$$

where d_i indicates the inside diameter of the tube. λ_s represents the thermal conductivity of superheated steam. Re_i and Pr_i are Reynolds number and Prandtl number of superheated steam, respectively.

The f_i from Eq. (5) is friction factor for turbulent flow in tubes and calculated as follows:

$$f_i = (1.82 \lg Re_i - 1.64)^{-2} \quad (6)$$

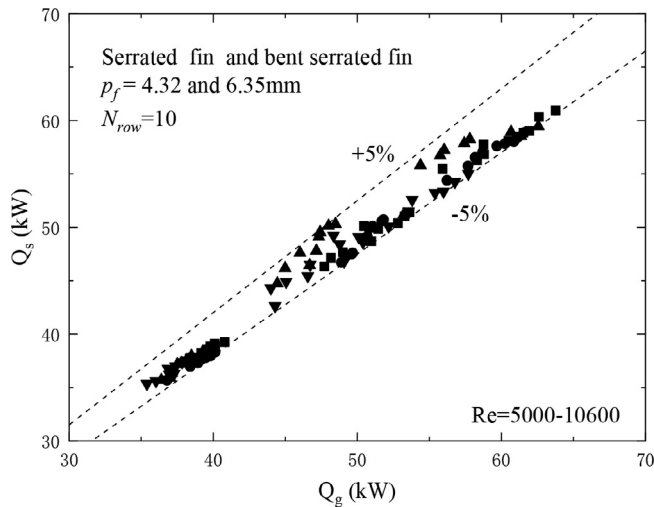


Fig. 6. Energy balance between the flue gas and steam.

The $Nu_{0,i}$ from Eq. (5) is the constant property case. In this experiment, the medium in the tube was steam, and the pressure and temperature will change during flowing in the tube. For variable property gasses, Sleicher revised the actual situation $Nu_{b,i}$ as follows [26]:

$$Nu_{b,i} = Nu_{0,i}(T_w/T_b)^m \quad (7)$$

where T_b and T_w indicate temperatures evaluated at the bulk and wall, respectively. The m is given by

$$m = -\log_{10}(T_w/T_b)^{1/4} + 0.3 \quad (8)$$

For better showing the heat transfer characteristic of flue gas side of different heat exchangers, the dimensionless parameter Colburn factor j was introduced, as shown below

$$j = \frac{Nu}{RePr^{1/3}} = \frac{\alpha_o}{\rho V_{max} C_p} Pr^{2/3} \quad (9)$$

The flue gas flow characteristics were evaluated by the friction factor f proposed by Kays, including inlet and outlet pressure losses [27–34]:

$$f = \left(\frac{A_{min}}{A_{tot}}\right) \left(\frac{\rho_g}{\rho_1}\right) \left[\frac{2\Delta P \rho_1}{G_c^2} - (1 + \sigma^2) \left(\frac{\rho_1}{\rho_2} - 1\right) \right] \quad (10)$$

where σ represents the minimum free flow area to frontal area ratio. A_{min} represents the minimum free flow area. A_{tot} means the total heat transfer area. G_c represents the flue gas mass flux at the minimum free flow area.

For Eq. (10), due to the small changes in the physical properties of the imported and exported flue gas in this experiment, entrance and exit effects are negligible, then f can be simplified as:

$$f = \frac{A_{min} \rho_g}{A_{tot}} \left(\frac{2\Delta P_1}{G_c^2}\right) \quad (11)$$

4. Results and discussion

Fig. 6 indicated that the energy unbalance between the gas and steam of heat exchangers was less than 5%, which was followed by the ANSI/ASHRAE 33 Standards. [27]. The energy balance between flue gas-side and steam-side was used to determine the performance of SSF and BSSF with different fin spacing. The heat transfer coefficient and heat transfer rate were drawn against Re to settle the heat exchange characteristic of all heat exchangers; the pressure drop against Re to set the flow characteristics. The Re depended on the base tube outside diameter (d_o). The comprehen-

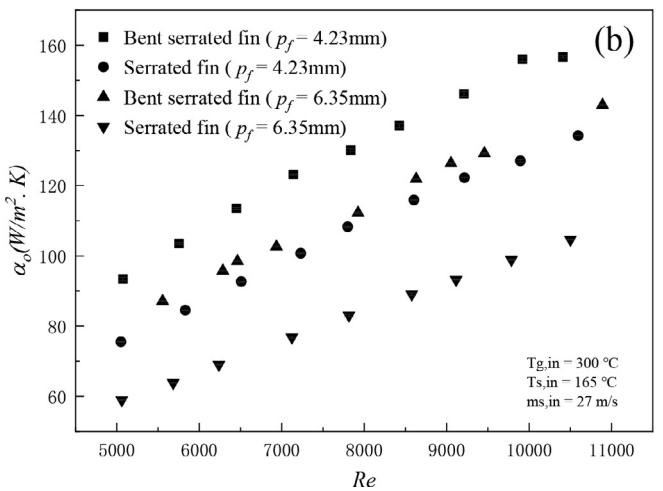
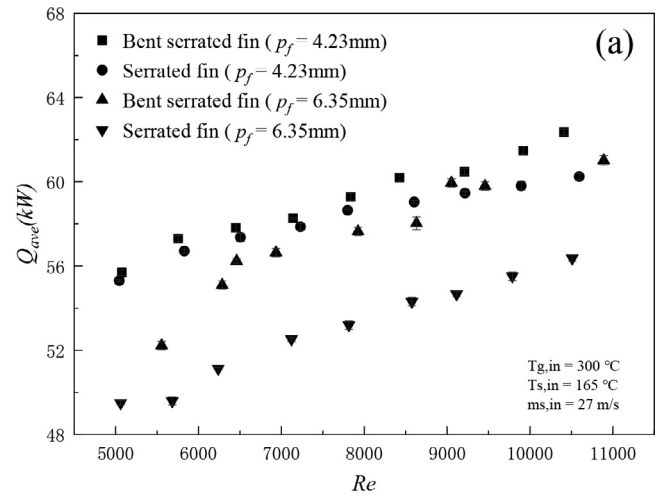


Fig. 7. Effect of fin type on the average heat transfer rate (a), gas side heat transfer coefficient (b) of spiral fin tube banks.

sive performance of different heat exchangers was fixed according to dimensionless parameters.

4.1. Experimental results on heat transfer characteristic of distinct heat exchangers

The relationship between the average heat transfer rate of flue gas and superheated steam, flue gas side heat transfer coefficient and Re ($Re = 5500 - 10,600$) were shown in Fig. 7, respectively.

The test illustrated that the heat transfer and heat transfer coefficient increased with increasing Re number. The increase in Re proved that the flue gas side flow has become turbulent, and the mixing is better promoted, resulting in better heat transfer performance. This phenomenon is universal for the four fin types tested in this paper.

For discontinuous fin types, Xu et al. [28] considered that discontinuous fin and staggered fin enhanced heat transfer performance due to the interruption in the airflow by different row structures, resulting in the flow and regeneration of the thermal boundary layer.

Comparing different fin types with the same fin pitch, BSSF has a higher heat transfer coefficient than SSF under the same heat transfer area and operating conditions. Fig. 7 shows that the heat transfer rate of the 4.23 mm BSSF was 0.17–2.95% more than that of SSF. The 6.35 mm BSSF heat exchange was 8.1–9.04% higher than that of the SSF. The gas side heat transfer coefficient of the

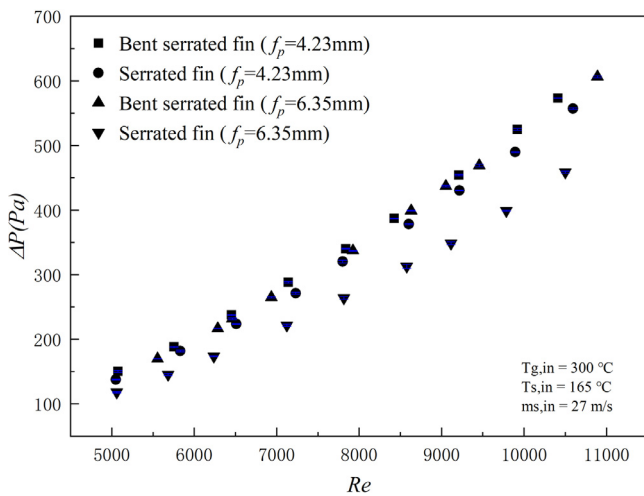


Fig. 8. Effect of fin type on the pressure drop of spiral fin tube banks.

4.23 mm BSSF was 19.98–24.52% (32.53–39.82% for 6.35 mm) more than that of SSF. The data showed that the twist and bend of the fin were the main reasons for the increased heat transfer capacity.

The heat transfer performance of the BSSF and the SSF of the 4.23 mm fin pitch were greater than that of the 6.35 mm fin pitch, respectively, when the fin types were the same. This was because the flow cannot be fully developed by reducing the fin pitch in this study. The existence of the tube bank enhanced heat transfer by generating longitudinal eddy currents and unstable and defective oscillating flows (Coanda effect). Therefore, a greater fin pitch may lead to a more stable flow and reduce the overall performance [29, 30]. At the same time, the larger fin pitch led to the smaller heat transfer area per unit length of the tube, which will also make the heat transfer performance of the larger pitch worse.

4.2. Experimental results on pressure drop

Fig. 8 shows the effect of fin-type on the pressure drop of the heat exchangers. As expected, the pressure drop increased with the increase of air Re. The reason was that when Re increased, the effect of inertial force was significantly enhanced. The airflow boundary layer was separated on the tube wall, forming a complex turbulent vortex, which can improve the heat transfer performance and increase the pressure drop.

Comparing the bent and unbent finned tubes with the same pitch, the pressure drop of 4.23 mm BSSF was 5.77–9.04% higher than that of SSF, and the pressure drop of 6.35 mm BSSF was 11.68–26.64% higher than that of SSF. This was in accordance with the conclusion above. This was because the distortion and bending of the fins improved the turbulence intensity on the flue gas side. At the same time, the minimum flow cross-sectional area (A_{min}) became smaller, which will also lead to the increasing of resistance.

The pressure drop was larger when the pitch was smaller when the fin structure was the same. This was because the decrease of the fin pitch increased the pressure blocking in the flow area. Li et al. [31] believed that the increase in fin pitch led to fewer fins per unit tube length, resulting in a larger cross-sectional area and lower wind speed, so the pressure drop was reduced.

4.3. The effect of superheated steam flow

Fig. 9 shows the effect of inlet steam flow rate on the heat transfer and resistance characteristics of 4.23 mm BSSF. In this paper, the inlet pressure was 0.4 MPa, and the inlet steam temper-

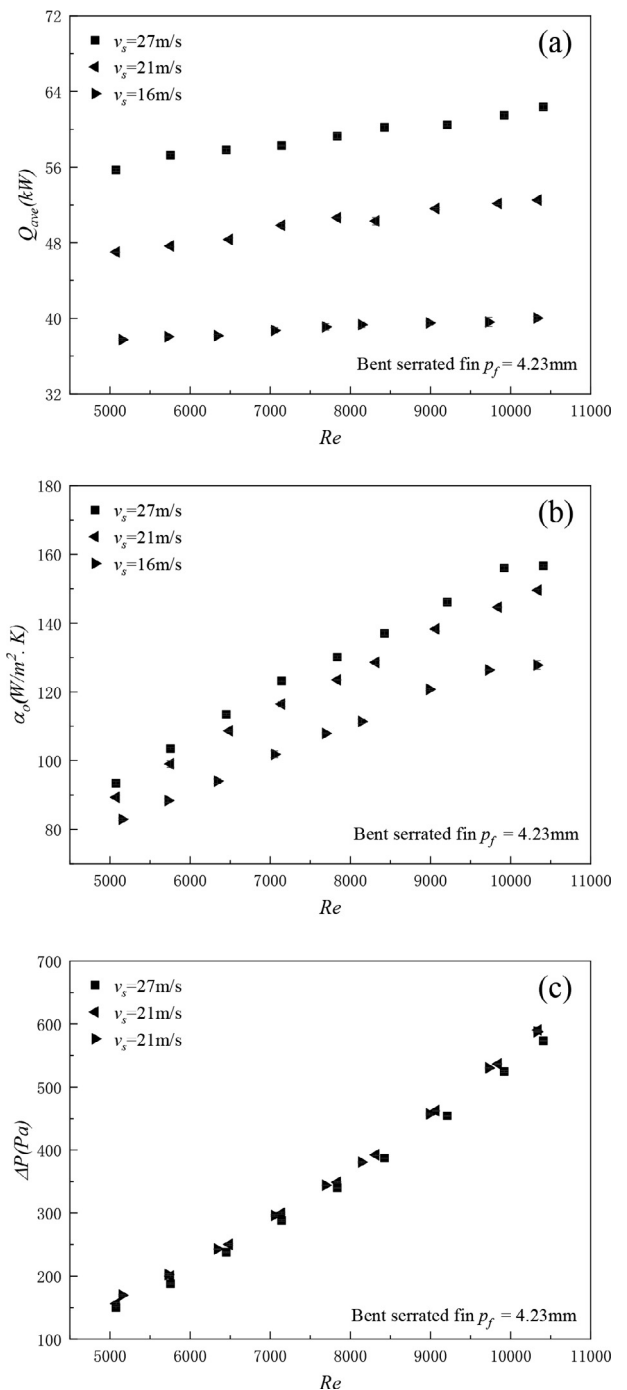


Fig. 9. Effect of inlet steam flow rate on the average heat transfer rate (a), gas side heat transfer coefficient (b) and pressure drop (c) of spiral fin tube banks.

ature was 165 °C. The inlet steam flow rates were set at 16 m/s, 21 m/s and 27 m/s, respectively. With the increase of inlet steam flow, the overall heat transfer coefficient and heat transfer coefficient on the external side increased. This was because with the rise in inlet steam flow rate, the total steam in the pipe has increased, and the heat absorption capacity was stronger. At the same time, the residence time of steam in the heat exchange tube turned shorter, and the heat absorption decreased, decreasing the temperature rise of steam in the tube. The increase of heat exchange temperature difference also led to the enhancement of heat exchange performance. Besides, the tube side convective heat transfer co-

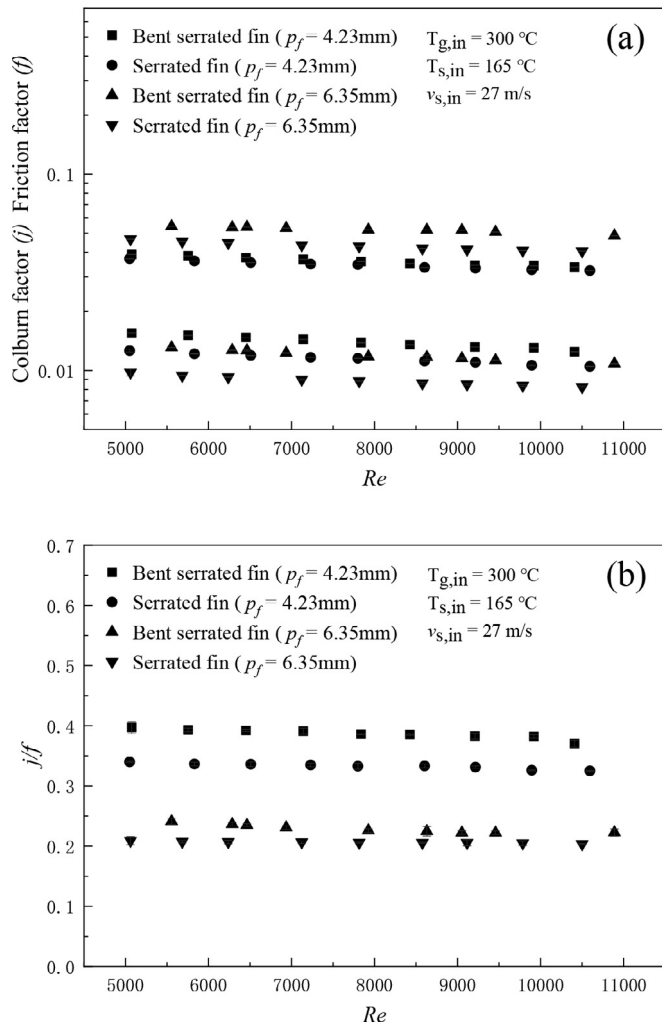


Fig. 10. Effect of fin type on (a) the Colburn factor and friction factor and (b) Colburn-Fanning factor ratio (j/f).

efficient increased with the increase of steam velocity. This phenomenon verified the point of this paper.

The change of inlet steam velocity had little effect on the pressure drop of flue gas outside the pipe. The steam velocity affected the resistance characteristics by affecting the thermophysical properties of flue gas, and its effect can be ignored.

4.4. Overall performances evaluation

In this study, the comprehensive performance of four heat exchangers was evaluated by dimensionless parameters j , f and j/f . As can be seen from Fig. 10(a), j and f of all heat exchangers decreased with the increase of Re as expected.

It can be seen that the j of BSSF at $4.23\text{ mm } p_f$ was greater than that of SSF. This may be because bent fins can enhance contact with flue gas. At the same time, the heat transfer characteristic of the flue gas wake on the leeward side of the fins may become stronger due to the distortion of the fins. At the same time, the smaller the fin pitch, the better the heat transfer performance. This was consistent with the previous experimental results.

It can be seen that f of BSSF at $4.23\text{ mm } p_f$ was 3.63–5.76% larger than SSF's, and f of BSSF at $6.35\text{ mm } p_f$ was 19.09–24.41% larger than SSF's. This may be because the twist of the fins increased the turbulence degree of the flue gas. At the same time, due to the twist of the fins, the minimum flow cross-sectional

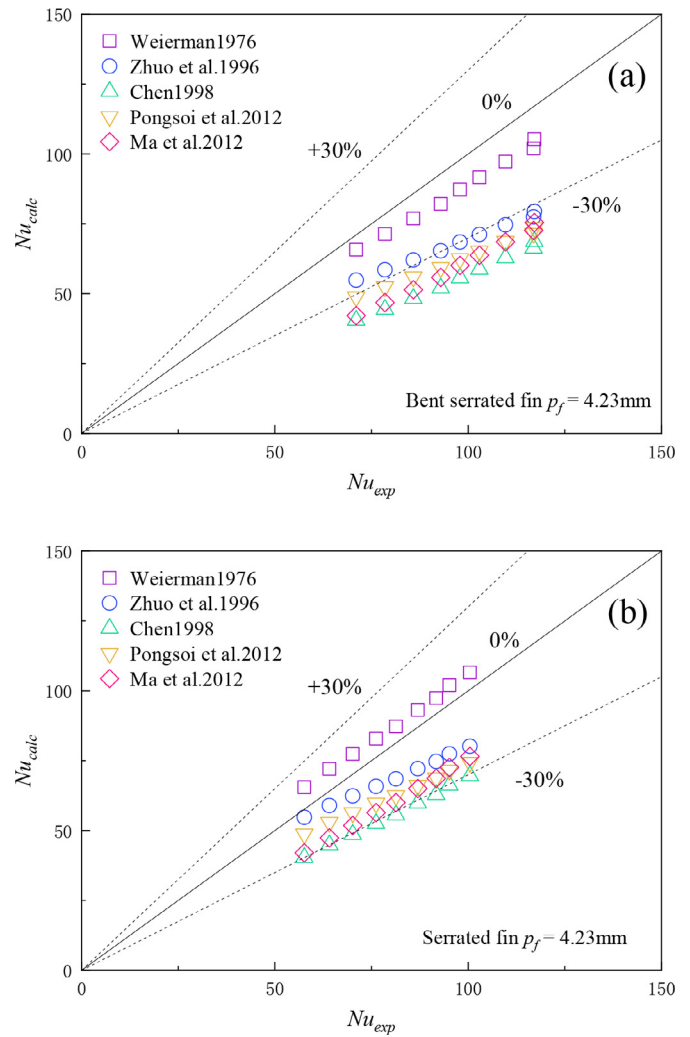


Fig. 11. Comparison between the heat transfer test data of (a) BSSF $p_f = 4.23\text{ mm}$ and (b) SSF $p_f = 4.23\text{ mm}$ and the predicted values calculated from previously published correlations.

area (A_{min}) became smaller. It can be seen from the Fig. 10(a) that when the fin types were the same, f with a larger fin pitch was higher than that with a smaller fin pitch. This was consistent with the experimental results of Parinya Pongsoi et al. [32]. According to Eq. (11), f was directly proportional to the ratio of the minimum free flow area to the total heat transfer area (A_{min} / A_{tot}) and inversely proportional to the gas mass flux in the minimum free flow area (G_c). Larger fin pitch increased A_{min} / A_{tot} , but reduced G_c . Under the combined action of the two, the f with a larger fin pitch became higher.

The previous results showed that the principle of BSSF was to make the hot flue gas fluid passing through the fins more disordered and produce more turbulence. This structure improved the heat transfer factor j , but also the friction factor f . Strengthening heat exchange efficiency, reducing energy consumption and improving overall performance were the industrial needs. Therefore, this paper introduced the overall evaluation standard j/f . It can be known from Fig. 10(b) that the j/f of 4.23 mm BSSF was 15.18–17.05% higher than that of SSF. The j/f of 6.35 mm BSSF was 7.43–15.23% greater than SSF's.

It was worth noting that the increase of j and f of 6.35 mm BSSF relative to SSF were higher than that of 4.23 mm , probably due to the small heat absorption of superheated steam. The disturbance on the flue gas side under the condition of 4.23 mm SSF has been

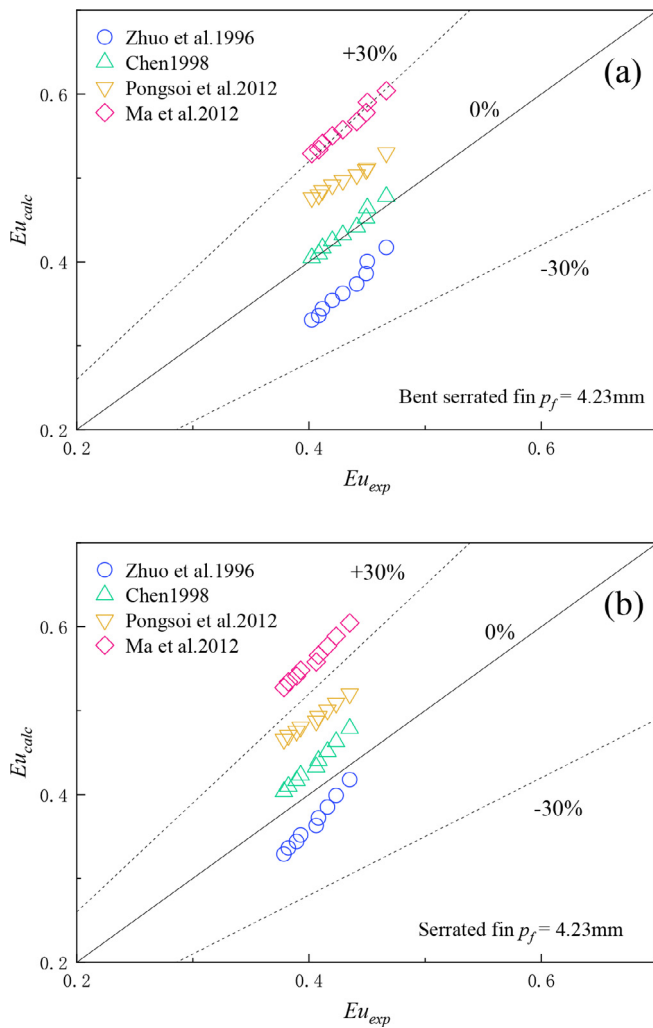


Fig. 12. Comparison between the pressure drop test of (a) BSSF $p_f = 4.23$ mm and (b) SSF $p_f = 4.23$ mm and the predicted values calculated from previously published correlations.

strong, so the twisted fins did not improve its heat exchange performance and resistance performance as much as that of 6.35 mm. Moreover, as the resistance of 6.35 mm BSSF increased too much compared with SSF, its comprehensive performance was not improved as much as that of 4.23 mm.

4.5. Comparisons of the correlations

Fig. 11 illustrates the comparison between the heat transfer measured data of $p_f = 4.23$ mm and the forecasting data calculated by formerly reported correlations (Weierman [13], Zhuo et al. [15], Chen [14], Pongsoi et al. [17], Ma et al. [16]).

It can be seen that the heat transfer correlation of Weierman [13] was the most consistent with the test data of BSSF, and the difference of all data was within 13%. The predicted Nu values of all the heat transfer correlations were less than that of BSSF. Zhuo et al. [15]'s heat transfer correlation showed the greatest degree of consistency with the tested result of SSF, with an average deviation of 7.4%. Compared with BSSF, the test data of SSF were more consistent with the heat transfer correlation of other studies. This may be because the distortion and dumping of BSSF fins improved the heat transfer performance, while the fins studied by Zhuo et al. [15] and Chen [14] were non-distorted fins.

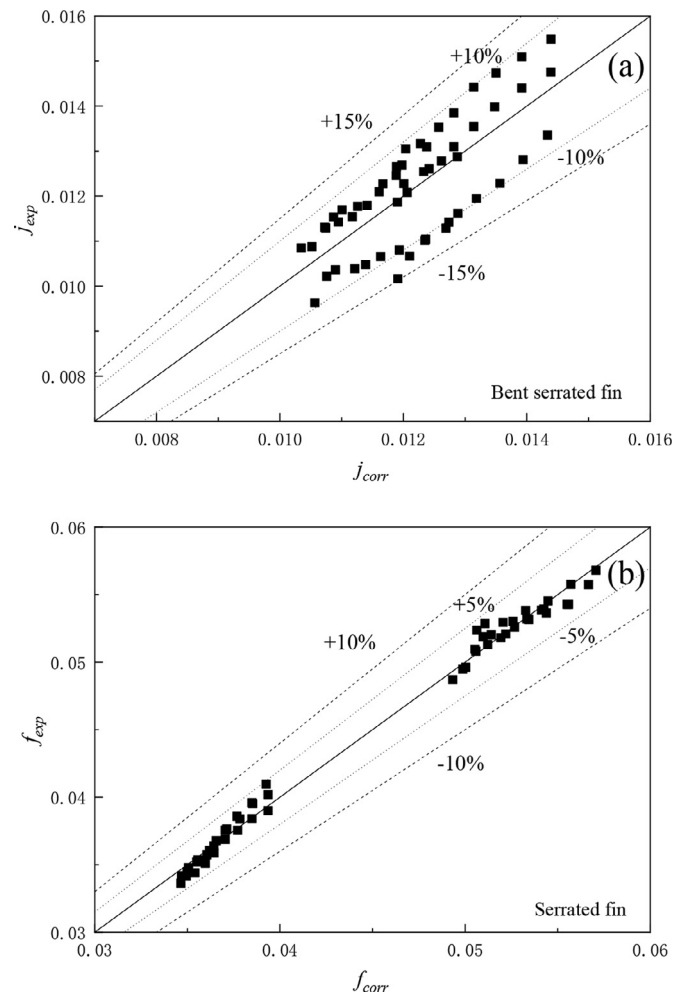


Fig. 13. Comparison empirical correlations with experimental data: (a) j and (b) f .

Fig. 12 suggests the comparison between the pressure drop measured results of $p_f = 4.23$ mm and the forecasting data according to formerly reported correlations. (Zhuo et al. [15], Chen [14], Pongsoi et al. [17], Ma et al. [16]).

Fig. 12(a) shows that the heat transfer correlation of Chen [14] was the most similar to the test data of BSSF, and the deviation was within 3.1%. It was worth noting that the Eu predicted by Zhuo et al. [15] was approached that of BSSF at low Re . With the increase of Re , the gap between them gradually becomes larger, showing that twist can strengthen the disturbance to the fluid at high Re , and the additional pressure drop caused by twisting increased with the increase of Reynolds number.

Fig. 12(b) shows that the heat transfer correlation of Chen [14] was the most consistent with the results of SSF, and the difference of all data was within 10%. However, the Eu of Ma et al. [16] was significantly higher than the test data, possibly due to the smaller fin pitch of the study by Ma et al. [16].

Finally, because few people have studied the twisted fin heat transfer of superheated steam in the tube, the correlation between j and f of BSSF under steam in the tube was proposed in this paper. As shown in [32], the influence of pipe row on j and f can be ignored. In this paper, the formula was fitted in the form of $j = aRe_{d_0}^b$ and $f = aRe_{d_0}^b$ according to Wang et al. [33], in which a and b were the empiric constant obtained by fitting the experimental data according to the least square method. During the experiment, j and f were affected by the fin pitch. Hence, the present relation expression for j and f factor were upgraded by including

the dimensionless p_f normalized by d_o . The formula was as follows:

$$j_{corr} = 0.07443Re^{-0.26651} \left(\frac{p_f}{d_o} \right)^{-0.31171} \quad (12)$$

$$f_{corr} = 1.0828Re^{-0.17751} \left(\frac{p_f}{d_o} \right)^{0.88954} \quad (13)$$

As presented in Fig. 13, the presented heat transfer and friction correlation Eqs. (12) and 13 can correlate 100% of the j and f within $\pm 15\%$ and $\pm 5\%$, respectively. The mean deviations of the proposed heat transfer and friction correlation were 6.2% and 1.3%, respectively. The correlation is suitable for: $p_f = 4.23\sim 6.35$ mm, $d_o = 32$ mm, $Re = 5500\sim 10,600$.

5. Conclusions

In this study, saw serrated spiral finned tubes with different fin types and fin pitch under the steam condition at high Reynolds number (5000–10,600) were experimentally studied. According to the test data, the following conclusions were drawn:

- (1) At the same Re number, the bent serrated spiral fin type improved the turbulence degree of flue gas side flow compared with that of the traditional serrated spiral fin. Thus, the heat exchange performance was improved, and the flue gas side resistance was increased. In this experiment, the heat transfer rate and pressure drop of heat exchangers with small fin pitch were greater than those with large fin pitch.
- (2) The steam side flow characteristics had a significant influence on the overall heat transfer characteristics of finned tubes. The fin side heat transfer coefficient increased with the increase of steam flow rate. But it had little effect on the resistance characteristics.
- (3) Through comprehensive performance evaluation, it was concluded that the j/f of 4.23 mm BSSF was 15.18–17.05% higher than that of SSF. The j/f of 6.35 mm BSSF was 7.43–15.23% greater than SSF's.

The comprehensive performance improvement of 4.23 mm BSSF relative to SSF was more significant than that with 6.35 mm fin pitch. Therefore, the economic benefit of 4.23 mm BSSF was higher.

(4) In this study, the experimental results were compared with the results of other researchers, and the correlation of serrated spiral fins j and f under the condition of steam in the tube was fitted. The average deviations were 6.2% and 1.3%, respectively.

Declaration of Competing Interest

The authors declare that they have no known competing financial interests or personal relationships that could have appeared to influence the work reported in this paper.

CRediT authorship contribution statement

Hao Zhou: Conceptualization, Methodology, Resources, Supervision, Project administration, Funding acquisition. **Tianxiao Liu:** Conceptualization, Methodology, Investigation, Data curation, Writing – original draft, Writing – review & editing, Visualization. **Fangzheng Cheng:** Investigation. **Dan Liu:** Investigation. **Yifan Zhu:** Investigation. **Weimei Ma:** Investigation.

Acknowledgments

This research did not receive any specific grant from funding agencies in the public, commercial, or not-for-profit sectors.

Supplementary materials

Supplementary material associated with this article can be found, in the online version, at doi:[10.1016/j.ijheatmasstransfer.2021.122333](https://doi.org/10.1016/j.ijheatmasstransfer.2021.122333).

Reference

- [1] S. Unger, M. Beyer, L. Szalinski, et al., Thermal and flow performance of tilted oval tubes with novel fin designs, Int. J. Heat Mass Transf. 153 (2020), doi:[10.1016/j.ijheatmasstransfer.2020.119621](https://doi.org/10.1016/j.ijheatmasstransfer.2020.119621).
- [2] Y. Kim, Y. Kim, Heat transfer characteristics of flat plate finned-tube heat exchangers with large fin pitch, Int. J. Refrig. 28 (6) (2005) 851–858, doi:[10.1016/j.ijrefrig.2005.01.013](https://doi.org/10.1016/j.ijrefrig.2005.01.013).
- [3] A. Okbaz, A. Pinarbasi, A.B. Olcay, Experimental investigation of effect of different tube row-numbers, fin pitches and operating conditions on thermal and hydraulic performances of louvered and wavy finned heat exchangers, Int. J. Therm. Sci. 151 (2020), doi:[10.1016/j.ijthermalsci.2019.106256](https://doi.org/10.1016/j.ijthermalsci.2019.106256).
- [4] J.-N. Zhang, M. Cheng, Y.-D. Ding, et al., Influence of geometric parameters on the gas-side heat transfer and pressure drop characteristics of three-dimensional finned tube, Int. J. Heat Mass Transf. 133 (2019) 192–202, doi:[10.1016/j.ijheatmasstransfer.2018.12.118](https://doi.org/10.1016/j.ijheatmasstransfer.2018.12.118).
- [5] Z.-Y. Chen, M. Cheng, Q. Liao, et al., Experimental investigation on the air-side flow and heat transfer characteristics of 3-D finned tube bundle, Int. J. Heat Mass Transf. 131 (2019) 506–516, doi:[10.1016/j.ijheatmasstransfer.2018.10.026](https://doi.org/10.1016/j.ijheatmasstransfer.2018.10.026).
- [6] T. Han, C.A. Wang, Q. Cao, et al., Investigation on heat transfer characteristics of the H-type finned tube in flue gas with high content of ash, Energy Procedia 105 (2017) 4680–4684, doi:[10.1016/j.egypro.2017.03.1014](https://doi.org/10.1016/j.egypro.2017.03.1014).
- [7] F.-L. Wang, S.-Z. Tang, Y.-L. He, et al., Heat transfer and fouling performance of finned tube heat exchangers: experimentation via on line monitoring, Fuel 236 (2019) 949–959, doi:[10.1016/j.fuel.2018.09.081](https://doi.org/10.1016/j.fuel.2018.09.081).
- [8] Z. Čarija, B. Franković, M. Perčić, et al., Heat transfer analysis of fin-and-tube heat exchangers with flat and louvered fin geometries, Int. J. Refrig. 45 (2014) 160–167, doi:[10.1016/j.ijrefrig.2014.05.026](https://doi.org/10.1016/j.ijrefrig.2014.05.026).
- [9] A. Nuntaphan, T. Kiatsiriroat, Thermal behavior of spiral fin-and-tube heat exchanger having fly ash deposit, Exp. Therm. Fluid Sci. 31 (8) (2007) 1103–1109, doi:[10.1016/j.expthermflusci.2006.11.007](https://doi.org/10.1016/j.expthermflusci.2006.11.007).
- [10] F. He, W. Cao, P. Yan, Experimental investigation of heat transfer and flowing resistance for air flow cross over spiral finned tube heat exchanger, Energy Procedia 17 (2012) 741–749, doi:[10.1016/j.egypro.2012.02.166](https://doi.org/10.1016/j.egypro.2012.02.166).
- [11] M. Lee, T. Kang, Y. Kim, Air-side heat transfer characteristics of spiral-type circular fin-tube heat exchangers, Int. J. Refrig. 33 (2) (2010) 313–320, doi:[10.1016/j.ijrefrig.2009.09.019](https://doi.org/10.1016/j.ijrefrig.2009.09.019).
- [12] E. Næss, Experimental investigation of heat transfer and pressure drop in serrated-fin tube bundles with staggered tube layouts, Appl. Therm. Eng. 30 (13) (2010) 1531–1537, doi:[10.1016/j.applthermaleng.2010.02.019](https://doi.org/10.1016/j.applthermaleng.2010.02.019).
- [13] C. Weierman, Correlations ease the selection of finned tubes, Oil Gas J. 74 (36) (1976) 94–100.
- [14] Chen Y., Cheng G., Experimental study on the heat transfer and flow resistance of serrated finned tube banks Chinese society of engineering, Thermophysics, Proceeding on Heat and Mass Transfer Academic Conference (1998) 47–52 Hefei.
- [15] N. Zhou, W. Jiang, J. Wang, et al., Heat transfer and flow resistance properties of helically segmented finned tube bank, East China Univ. Technol. 18 (1) (1996) 23–26, doi:[10.13255/j.cnki.jusst.1996.01.004](https://doi.org/10.13255/j.cnki.jusst.1996.01.004).
- [16] Y. Ma, Y. Yuan, Y. Liu, et al., Experimental investigation of heat transfer and pressure drop in serrated finned tube banks with staggered layouts, Appl. Therm. Eng. 37 (2012) 314–323, doi:[10.1016/j.applthermaleng.2011.11.037](https://doi.org/10.1016/j.applthermaleng.2011.11.037).
- [17] P. Pongsoi, S. Pikulkajorn, C.-C. Wang, et al., Effect of number of tube rows on the air-side performance of crimped spiral fin-and-tube heat exchanger with a multipass parallel and counter cross-flow configuration, Int. J. Heat Mass Transf. 55 (4) (2012) 1403–1411, doi:[10.1016/j.ijheatmasstransfer.2011.09.064](https://doi.org/10.1016/j.ijheatmasstransfer.2011.09.064).
- [18] A. Nuntaphan, T. Kiatsiriroat, C.C. Wang, Heat transfer and friction characteristics of crimped spiral finned heat exchangers with dehumidification, Appl. Therm. Eng. 25 (2–3) (2005) 327–340, doi:[10.1016/j.applthermaleng.2004.05.014](https://doi.org/10.1016/j.applthermaleng.2004.05.014).
- [19] A. Nuntaphan, T. Kiatsiriroat, C.C. Wang, Air side performance at low Reynolds number of cross-flow heat exchanger using crimped spiral fins, Int. Commun. Heat Mass Transfer 32 (1–2) (2005) 151–165, doi:[10.1016/j.icheatmasstransfer.2004.03.022](https://doi.org/10.1016/j.icheatmasstransfer.2004.03.022).
- [20] S. Xu, Direct calculation of flue gas properties, J. Suzhou Institute of Silk Textile Technol. 19 (3) (1999) 32–36.
- [21] W. Wagner, R.J. Cooper, The IAPWS industrial formulation 1997 for the thermodynamic properties of water and steam, J. Eng. for Gas Turbines Power (2000), doi:[10.1115/1.483186](https://doi.org/10.1115/1.483186).
- [22] S. Yang, W. Tao, Heat Transfer, 4th ed, Higher Education Press, Beijing, 2006.
- [23] V. Gnielinski, On heat transfer in tubes, Int. J. Heat Mass Transf. 63 (2013) 134–140, doi:[10.1016/j.ijheatmasstransfer.2013.04.015](https://doi.org/10.1016/j.ijheatmasstransfer.2013.04.015).
- [24] X. Ma, G. Ding, Y. Zhang, et al., Airside characteristics of heat, mass transfer and pressure drop for heat exchangers of tube-in hydrophilic coating wavy fin under dehumidifying conditions, Int. J. Heat Mass Transf. 52 (19–20) (2009) 4358–4370, doi:[10.1016/j.ijheatmasstransfer.2009.03.066](https://doi.org/10.1016/j.ijheatmasstransfer.2009.03.066).

- [25] H. Zhou, D. Liu, Q. Sheng, et al., Research on gas side performance of staggered fin-tube bundles with different serrated fin geometries, *Int. J. Heat Mass Transf.* 152 (2020), doi:[10.1016/j.ijheatmasstransfer.2020.119509](https://doi.org/10.1016/j.ijheatmasstransfer.2020.119509).
- [26] C.A. Sleicher, M.W. Rouse, A convenient correlation for heat transfer to constant and variable property fluids in turbulent pipe flow, *Int. J. Heat Mass Transf.* 18 (5) (1975) 677–683. doi:[10.1016/0017-9310\(75\)90279-3](https://doi.org/10.1016/0017-9310(75)90279-3).
- [27] Methods of testing forced-circulation air-cooling and air-heating coils: ASHRAE 33-2016. (2016).
- [28] C. Xu, L. Yang, L. Li, et al., Experimental study on heat transfer performance improvement of wavy finned flat tube, *Appl. Therm. Eng.* 85 (2015) 80–88, doi:[10.1016/j.applthermaleng.2015.02.024](https://doi.org/10.1016/j.applthermaleng.2015.02.024).
- [29] C.-W. Lu, J.-M. Huang, W.C. Nien, et al., A numerical investigation of the geometric effects on the performance of plate finned-tube heat exchanger, *Energy Convers. Manage.* 52 (3) (2011) 1638–1643, doi:[10.1016/j.enconman.2010.10.026](https://doi.org/10.1016/j.enconman.2010.10.026).
- [30] P. Pongsoi, S. Pikulkajorn, S. Wongwises, Effect of fin pitches on the optimum heat transfer performance of crimped spiral fin-and-tube heat exchangers, *Int. J. Heat Mass Transf.* 55 (23–24) (2012) 6555–6566, doi:[10.1016/j.ijheatmasstransfer.2012.06.061](https://doi.org/10.1016/j.ijheatmasstransfer.2012.06.061).
- [31] X. Li, D. Zhu, J. Sun, et al., Air side heat transfer and pressure drop of H type fin and tube bundles with in line layouts, *Exp. Therm. Fluid Sci.* 96 (2018) 146–153, doi:[10.1016/j.expthermflusci.2018.02.029](https://doi.org/10.1016/j.expthermflusci.2018.02.029).
- [32] P. Pongsoi, P. Promoppatum, S. Pikulkajorn, et al., Effect of fin pitches on the air-side performance of L-footed spiral fin-and-tube heat exchangers, *Int. J. Heat Mass Transf.* 59 (2013) 75–82, doi:[10.1016/j.ijheatmasstransfer.2012.11.071](https://doi.org/10.1016/j.ijheatmasstransfer.2012.11.071).
- [33] C.-C. Wang, W.-H. Tao, C.-J. Chang, An investigation of the airside performance of the slit fin-and-tube heat exchangers, *Int. J. Refrig.* 22 (8) (1999) 595–603, doi:[10.1016/S0140-7007\(99\)00031-6](https://doi.org/10.1016/S0140-7007(99)00031-6).
- [34] W.M. Kays, A. London, *Compact Heat Exchangers*, third ed., McGraw-Hill, New York, 1984.